JOURNAL OF MATERIALS SCIENCE 22 (1987) 1687–1693

Characterization of hot-pressed silicon nitride-based materials by microhardness measurements

G. N. BABINI, A. BELLOSI, C. GALASSI
Research Institute for Ceramics Technology, CNR, Faenza, Italy

The microhardness of Si_3N_4-based materials may be related to their phase and chemical compositions and to microstructural parameters such as porosity, grain size and secondary phases. By reducing the amount of intergranular phase, the microhardness may reach values up to $HV_{500} = 3000\,kg\,mm^{-2}$. Moreover, a comparison among different materials must include the microhardness tests in a wide range of values of the applied load. The relation $d^n = B_1 + B_2 d^2$, obtained from those of Meyer and Kick, gives two constants: B_1 may represent one class of materials and B_2 is specific for each single material.

1. Introduction

At present there are few hardness data on Si_3N_4-based materials, even though this characteristic is of primary importance for materials considered for use in cutting tools and other applications. The microhardness of silicon nitride ceramics decreases with increasing test load [1–6], as expected for hard, brittle ceramics. There is a close connection [7, 8] between the microhardness and the chemical composition, textural and microstructural characteristics of the materials. The present work represents a study of these relationships based on data obtained from microhardness tests on hot-pressed silicon nitride materials in various systems: Si_3N_4–MgO, Si_3N_4–MgO–ZrO_2, Si_3N_4–CeO_2, Si_3N_4–Y_2O_3–SiO_2, Si_3N_4–Al_2O_3 and Si_3N_4–Al_2O_3–ZrO_2.

Reference to Meyer's relationship [9–12] turns out to be very effective as well as Kick's equation [13], modified according to Hays and Kendall [14], and attempts are made to correlate the constants involved in the empirical relationships of some microstructural parameters of the materials.

2. Experimental procedure

Starting compositions, hot-pressing conditions and some microstructural characteristics relevant for microhardness in the tested materials are shown in Tables I to IV. Details of the experimental procedures for the fabrication of the materials, of the densification mechanisms and of some specific characterizations (microstructure, oxidation resistance, thermal expansion behaviour etc.) have been reported elsewhere [15–24]. Small samples of Si_3N_4 were mounted in resin, ground and polished with diamond paste up to 0.1 μm. The Vickers microhardness was measured with a Zwick 3212 microdurometer, equipped with a detector and on-line with a computer. A loading rate below $0.3\,mm\,sec^{-1}$ for a duration of 10 sec was used for each impression. Tests were performed with loads between 200 and 1000 g. Care was taken to make indentations only on those areas which had no visible pores.

3. Results and discussion

In Tables I to IV the Vickers hardness of the various materials obtained with a 500 g load is reported. In Table V the variation with load of hardness and of indentation size for samples of the Si_3N_4–MgO, Si_3N_4–Al_2O_3 and Si_3N_4–Al_2O_3–ZrO_2 systems are shown.

3.1. Microhardness dependence on the microstructural parameters

When the hardness data in Tables II and III are plotted as a function of density (Fig. 1), a linear relationship is seen to exist among the samples of the same starting compositions.

In Fig. 2 is shown the microhardness variation with residual α-Si_3N_4 phase of hot-pressed materials in the systems Si_3N_4–Al_2O_3, Si_3N_4–Al_2O_3–ZrO_2 and Si_3N_4–MgO. The direct improvement of microhardness with the amount of α-Si_3N_4 phase agrees with the experimental results reported by Parr *et al.* [1] and Chakraborty and Mukerji [5] who reported that the basal planes of α-Si_3N_4 are about 28% harder than those of β-Si_3N_4 single crystals under identical microhardness testing conditions. According to the behaviour reported by Coe *et al.* [3] an inverse relation of hardness against mean grain size can be observed as in Fig. 3.

3.2. The effects of chemical additives on microhardness

The characteristics of the secondary phase strongly affect all the thermochemical properties of Si_3N_4-based materials; regarding the microhardness, it generally decreases with an increase in the amount of secondary phases, but it is also strictly linked with the

0022–2461/87 $03.00 + .12

TABLE I Materials, compositions and some microstructural parameters for the Si_3N_4–CeO_2 and Si_3N_4–CeO_2–SiO_2 systems and their Vickers hardness HV_{500}. All the samples were hot-pressed at 1650° C and P = 29.9 MPa

Sample	Additions to Si_3N_4* (wt %)	Relative density (%)	Intergranular phase volume (vol %)	Silicates of intergranular phase (vol %)	HV_{500} (kg mm^{-2})
1Ce	1 CeO_2	92.5	6.3	2.7	1899
2.5Ce1	2.5 CeO_2	95.0	6.5	3.8	1623
2.5Ce2	2.5 CeO_2	98.0	6.5	3.8	1840
5Ce1	5.0 CeO_2	93.9	6.9	5.5	1490
5Ce2	5.0 CeO_2	98.7	6.9	5.5	1734
5Ce3	5.0 CeO_2	98.2	6.9	5.5	1352
5Ce4	5.0 CeO_2	91.2	6.9	5.5	1618
5Ce5	5.0 CeO_2	89.9	6.9	5.5	1352
5Ce6	5.0 CeO_2	89.1	6.9	5.5	1505
7.5Ce1	7.5 CeO_2	99.2	7.3	7.3	1640
7.5Ce2	7.5 CeO_2	97.9	7.3	7.3	1590
10Ce1	10 CeO_2	90.8	8.8	8.8	1138
10Ce2	10 CeO_2	95.8	8.8	8.8	1352
15Ce1	15 CeO_2	99.8	11.8	11.8	1786
15Ce2	15 CeO_2	100.0	11.8	11.8	1584
20Ce1	20 CeO_2	100.0	14.9	14.9	1685
20Ce2	20 CeO_2	100.0	14.9	14.9	1732
20Ce3	20 CeO_2	100.0	14.9	14.9	1773
CeSi	6.6 CeO_2 + 7 SiO_2	99.0	32.7	6.4	1698

*Si_3N_4: AME Refractory grade.

TABLE II Compositions, hot-pressing conditions, some microstructural parameters and Vickers microhardness at 500 g load for the Si_3N_4–Al_2O_3, Si_3N_4–Al_2O_3–ZrO_2 and Si_3N_4–MgO systems

Sample	Additions to Si_3N_4* (wt %)	Hot-pressing conditions (P = 34.4 MPa)		Mean grain size (μm)	Residual α-phase (%)	Relative density (%)	HV_{500} (kg mm^{-2})
		T (° C)	t (min)				
AZ1	5 Al_2O_3† + 12 ZrO_2‡	1580	30	0.48	68.0	95	3038
AZ2	5 Al_2O_3 + 12 ZrO_2	1540	30	–	87.0	93	2394
AZ3	5 Al_2O_3 + 12 ZrO_2	1650	60	0.72	28.0	97	2498
AZ4	5 Al_2O_3 + 12 ZrO_2	1650	120	0.85	26.0	97	2132
AZ5	5 Al_2O_3 + 12 ZrO_2	1650	220	0.90	8.0	97	2086
AZ6	5 Al_2O_3 + 12 ZrO_2	1700	120	1.0	6.5	98	1950
A1	5 Al_2O_3†	1650	60	0.56	69.0	95	3009
A2	5 Al_2O_3	1650	120	0.85	40.0	98	2408
A3	5 Al_2O_3	1650	220	0.93	13.5	99	2162
M1	3MgO§	1600	10	0.55	78.0	99.6	2642
M2	3MgO	1600	60	0.80	48.0	100	2115
M3	3MgO	1600	90	0.88	42.0	100	2086

*Si_3N_4: LC10-Stark,† Al_2O_3: Alcoa, ‡ ZrO_2: Harshaw, § MgO: C. Erba.

TABLE III Materials, compositions, density, amount of the intergranular phase after hot-pressing for the Si_3N_4–Y_2O_3–SiO_2 system and their Vickers hardness HV_{500}. All the samples were hot-pressed at T = 1700° C and P = 29.9 MPa; Type A: little sample, ϕ = 2.5 cm; Type B: large sample, ϕ = 6 cm

Sample	Composition (mol %)			Relative density (%)	Intergranular phase (vol %)	Silicates of intergranular phase (vol %)	HV_{500} (kg mm^{-2})
	Si_3N_4*	SiO_2	Y_2O_3				
1Y2A	72.07	17.44	9.08	98.0	23.9	19.9	1635
1Y2B	72.07	17.44	9.08	96.3	23.9	19.9	1452
1Y5A	72.08	21.98	4.52	99.1	34.3	11.3	1736
1Y5B	72.08	21.98	4.52	97.8	34.3	11.3	1614
1Y3B	72.05	19.77	6.81	98.2	30.1	15.8	1686
1Y2B	77.33	13.85	7.30	97.7	19.0	16.1	1650
2Y3B	77.32	15.69	5.47	98.8	23.9	12.6	1766
2Y5B	77.32	17.52	3.65	98.2	27.2	9.4	1863
4Y3A	88.04	7.46	2.77	97.6	11.8	7.1	1782
4Y3B	88.04	7.46	2.77	85.3	11.8	7.1	1121

*Si_3N_4: AME Refractory grade.

TABLE IV Compositions, relative density and Vickers microhardness at 500 g load for materials hot-pressed in the system Si_3N_4–MgO–ZrO_2

Sample	Additions to Si_3N_4* (wt %)	Relative density (%)	HV_{500} (kg mm^{-2})
Z12-1	3 MgO† 12 ZrO_2‡	97	2023
Z17-1	3 MgO 17 ZrO_2	95	1957
Z22-1	3 MgO 22 ZrO_2	94	1909
Z27-1	3 MgO 27 ZrO_2	94	1530
Z12-9	3 MgO 12 ZrO_2§	98	1981
Z17-9	3 MgO 17 ZrO_2	95	1972
Z22-9	3 MgO 22 ZrO_2	95	1944
Z27-9	3 MgO 27 ZrO_2	94	1838

*Si_3N_4: LC10 Stark, †MgO: C. Erba, ‡ZrO_2: Merck (1 h milled, 3.9 m^2 g^{-1} specific surface area BET), §ZrO_2: Merck (9 h milled, 8.0 m^2 g^{-1} specific surface area BET).

type (crystallinity, compositions) of the secondary phases. Therefore the microhardness depends on the starting composition and on the chemical reactions between Si_3N_4, additives and impurities during hot pressing. The several systems examined allow the investigation of the changes in microhardness for Si_3N_4 ceramics prepared with different polyphase microstructures. For the following analyses only materials with relative density in the range 98 to 100% are considered in order to avoid the effect of the porosity.

3.2.1. Materials of the Si_3N_4–CeO_2 system

The variation of microhardness with the amount of CeO_2 in the starting composition is shown in Fig. 4. The crystalline intergranular phase of these materials is primarily constituted by cerium orthosilicate, $Ce_{4.67}(SiO_4)_3O$ [21], with traces of silicates of the additive and the impurities of the starting Si_3N_4 powder. With low additive contents (up to ~10 wt %), the composition of the intergranular phase is constant and mainly glassy, consequently the microhardness decreases when the amount of intergranular phase is increased. With higher additive contents (10 to 20 wt %) the amount of crystalline cerium

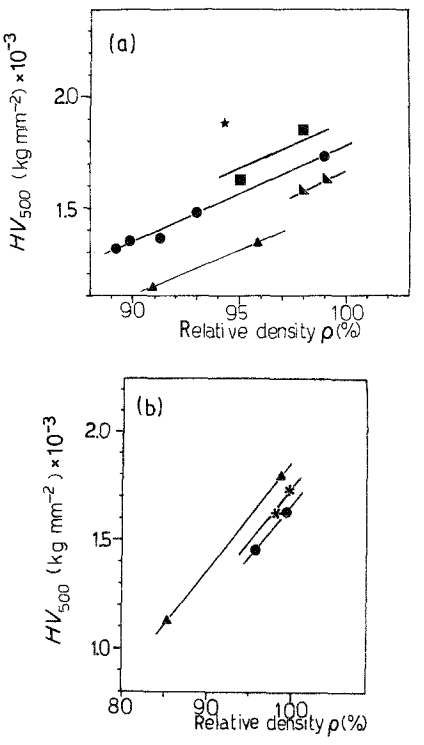

Figure 1 Vickers microhardness variation with density. (a) Si_3N_4–CeO_2 materials: (★) 1Ce, (■) 2.5Ce, (●) 5Ce, (◣) 7.5Ce, (▲) 10Ce. (b) Si_3N_4–Y_2O_3–SiO_2 materials: (●) 1Y2, (*) 1Y3, (▲) 4Y3.

silicates increases, due to the relevant quantity of liquid phase during hot pressing which promotes the crystallization of the secondary phases and causes a relative increase of microhardness. The sample CeSi, with high addition of SiO_2, exhibits a microhardness value that seems to depend only on the amount of CeO_2, and consequently of cerium orthosilicate.

It could therefore be concluded that microhardness does not depend only on the amount of secondary phases, but primarily on their type (glassy or crystalline) and composition (silicate or silicon oxynitride).

3.2.2. Materials of the Si_3N_4–Y_2O_3–SiO_2 system

The types and amounts of secondary phases are related to the starting compositions (Table III), and

TABLE V The variation of indentation size and hardness with Si_3N_4 sample and load; the nature of the Si_3N_4–Al_2O_3 and Si_3N_4–Al_2O_3–ZrO_2 materials are reported in Table I, and of the Si_3N_4–MgO sample in Table II

Sample	200 g load		400 g load		500 g load		700 g load		800 g load		1000 g load	
	d* (μm)	HV_{200} (kg mm^{-2})	d (μm)	HV_{400} (kg mm^{-2})	d (μm)	HV_{500} (kg mm^{-2})	d (μm)	HV_{700} (kg mm^{-2})	d (μm)	HV_{800} (kg mm^{-2})	d (μm)	HV_{1000} (kg mm^{-2})
AZ1	10.3	3459	16.1	3084	17.0	3038	22.5	2511	24.9	2411	28.4	2292
AZ2	10.7	3205	16.5	2572	19.6	2394	24.5	2152	26.5	2106	30.6	1966
AZ3	11.0	3024	16.8	2628	19.2	2498	24.0	2260	25.9	2206	29.4	2158
AZ4	11.8	2650	17.7	2350	20.9	2132	25.3	2026	27.3	1938	31.9	1822
AZ5	12.1	2551	18.4	2179	21.1	2086	25.6	1965	28.3	1845	33.2	1686
AZ6	12.5	2364	18.9	2079	21.7	1950	26.4	1857	28.8	1794	33.5	1655
A1	10.5	3416	15.4	3157	17.6	3009	22.6	2580	25.7	2482	28.1	2336
A2	11.7	2708	17.3	2456	19.6	2408	24.0	2256	25.7	2250	29.1	2192
A3	11.7	2710	17.5	2333	20.7	2162	24.4	2178	25.9	2167	29.2	2156
M1	11.0	3075	16.4	2761	18.7	2642	23.0	2448	25.0	2394	28.3	2309
M2	11.8	2677	18.2	2250	20.9	2115	24.9	2081	26.8	2063	30.4	2012
M3	12.3	2465	18.7	2106	31.7	2086	25.0	2077	26.9	2052	31.1	1908

*d = indentation diagonal.

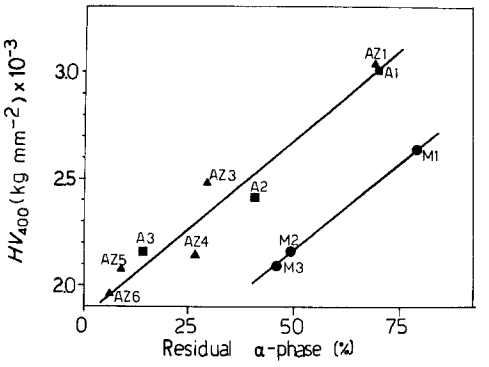

Figure 2 Relation between the Vickers microhardness and residual Si_3N_4 phase for materials of (■) Si_3N_4–Al_2O_3, (▲) Si_3N_4–Al_2O_3–ZrO_2 and (●) Si_3N_4–MgO systems.

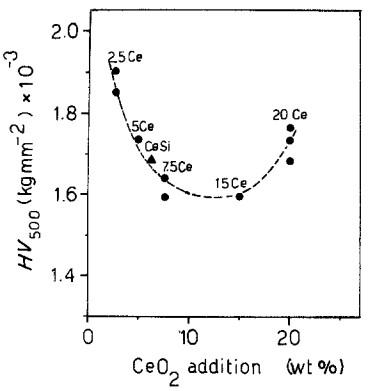

Figure 4 Relation between the Vickers microhardness and the amount of CeO_2 in the starting compositions of the Si_3N_4–CeO_2 materials. Sample CeSi refers to a material with the addition of 6.6 wt % CeO_2 and 7.0 wt % SiO_2. $98 \leqslant \varrho \leqslant 100$.

X-ray diffraction analysis shows the presence of crystalline secondary phases such as yttrialite, miserite, $Y_2Si_2O_7$ and Si_2N_2O [20, 23, 24]. In order to identify the samples, the notation xYz has been used, in which $x = 1$ or 2 indicates different Si_3N_4 contents, and $z = 1$, 3, 5 gives the approximate SiO_2/Y_2O_3 ratio. For the same Si_3N_4 content, the hardness of these materials (a) increases with a rise in the amount of SiO_2 (Fig. 5a), and (b) decreases with an increase in the amount of Y_2O_3 (Fig. 5b). The slopes of the lines in Fig. 5b indicate a more rapid hardness variation of the $2Yz$ compared to the $1Yz$ samples, i.e. the influence of yttria addition is greater when lowering the total amount of the additives (Table III). This behaviour causes a microhardness increase with the SiO_2/Y_2O_3 ratio (full lines in Fig. 6a) corresponding to higher amounts of Si_2N_2O in the intergranular phase, and to a higher crystallinity of the secondary phases. Maintaining equal values in the SiO_2/Y_2O_3 ratio (dashed lines in Fig. 6a), an inverse relationship can be observed between hardness and the volume of intergranular phase. Referring to the yttrium silicates in the intergranular phase, an inverse relationship results between its amount and microhardness (Fig. 6b).

3.2.3. Materials of the Si_3N_4–MgO and Si_3N_4–MgO–ZrO_2 systems

In hot-pressed materials with 3 wt % MgO as densification aid (Table II and Figs 2 and 3) higher microhardness values than those of the systems previously examined were detected, even though depending on the percentage of α-Si_3N_4 and on the mean grain size. This could be due to a low quantity of intergranular phase (~ 6 vol % of glassy silicates). The addition of various amounts of ZrO_2 (as a toughening phase) slightly changes the intergranular phase content, because the ZrO_2 particles are present with a discrete and random distribution and only a few of them are involved in the formation of the intergranular phase [22]. The variation of hardness with ZrO_2 addition is shown in Fig. 7.

3.2.4. Materials of the Si_3N_4–Al_2O_3 and Si_3N_4–Al_2O_3–ZrO_2 systems

These ceramics register the highest microhardness among the various materials tested, and these values (Table II and Figs 2 and 3) are higher than ever reported both for single Si_3N_4 crystals (HV_{500} = 2000 kg mm^{-2} on the basal plane [5] and for polycrystalline Si_3N_4-based materials [5, 7]; this phenomenon could be explained on the basis of the reaction between Al_2O_3 and Si_3N_4 during hot pressing causing the formation of a β′-sialon solid solution. Therefore a very scarce intergranular phase is present in the hot-pressed material, and a large degree of covalent bonding would be maintained in the Si_3N_4 crystal structure. The addition of zirconia does not appreciably affect the microhardness.

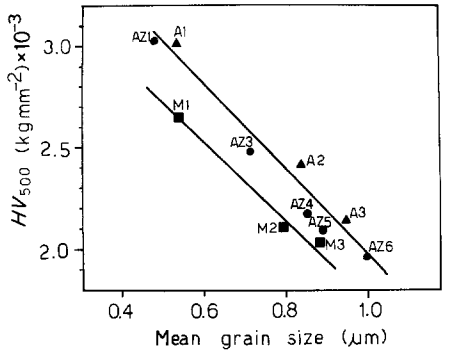

Figure 3 The Vickers microhardness against mean grain size for materials of (▲) Si_3N_4–Al_2O_3, (●) Si_3N_4–Al_2O_3–ZrO_2 and (■) Si_3N_4–MgO systems.

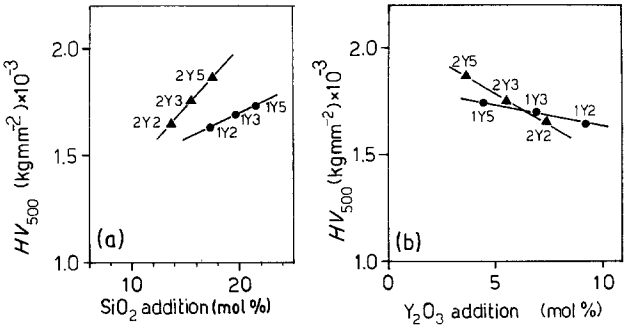

Figure 5 Variation of Vickers microhardness with (a) the amount of SiO_2 and (b) the amount of Y_2O_3 in the starting compositions of the Si_3N_4–Y_2O_3–SiO_2 materials. $97 \leqslant \varrho \leqslant 99$.

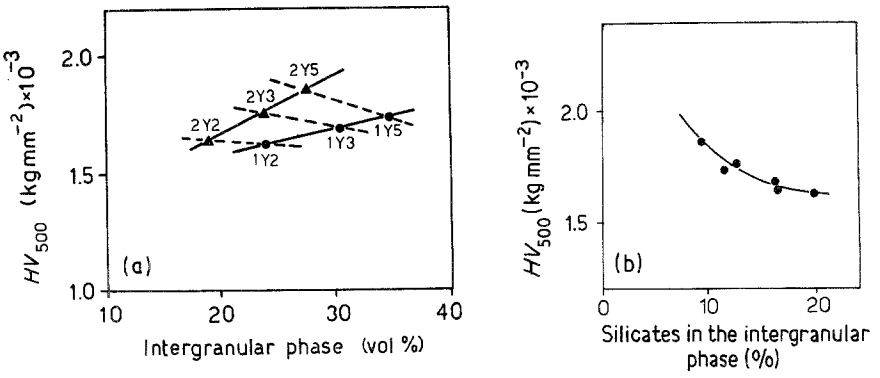

Figure 6 Relation between the Vickers microhardness and (a) intergranular phase volume, (b) the amount of yttrium silicates in the intergranular phase, for the Si_3N_4–Y_2O_3–SiO_2 materials. $97 \leqslant \varrho \leqslant 99$.

3.3. Microhardness analysis according to the Meyer and Kick relationships

3.3.1. Variation of microhardness with applied load

In Fig. 8 the microhardness values of the Si_3N_4–MgO, Si_3N_4–Al_2O_3 and Si_3N_4–Al_2O_3–ZrO_2 materials examined in relation to the applied load are shown. The general behaviour is typical of hard and brittle ceramics. The materials (M3, M2, A3, AZ2, AZ5) also show a higher variation of microhardness in the lower load range. They have higher contents of the residual α-Si_3N_4 phase, this being a phase with a microhardness higher than the β-Si_3N_4 phase [1, 5]. Beyond a given value of the load the above-mentioned difference between the two phases becomes uninfluential.

3.3.2. Analysis according to the Meyer relationship

The Meyer line is defined by the linear relationship

$$\log P = n \log d + \log a \qquad (1)$$

where P is the load (g) and d the average length (μm) of the indentation diagonal; n, the slope of the Meyer line, is a constant which is characteristic of the material and a is a constant. Meyer lines were drawn for the loads and indentation diameters listed in Table V. The relationship was proved sufficiently suitable for the representation of the experimental data. The computed values for n vary between 1.50 and 1.77, depending on the material. Since that value is lower than 2, the ceramics considered have no capacity for work-hardening, that is, they belong to the class of hard and brittle materials. Chakraborty and Mukerji [5] have shown that the Meyer constants may be related to the residual porosity; this was also found for the materials examined, whatever the starting composition (Fig. 9). There is reason to believe that the slope of the Meyer lines, n, can give a better indication of the porosity of Si_3N_4-based materials than individual Vickers hardness measurements. This can be ascribed to the influence of the nature of the Si_3N_4 phases and of the chemical additives, which has a much greater effect on the microhardness values than on the slope of the Meyer line as reported by Chakraborty and Mukerji [5]. A relationship is also evident between the Meyer constant and the grain size (Fig. 10) but in this case the data for each system fit separately. The constant a is another characteristic of the materials. It exhibits a dependence on the mean grain size in relation to the starting composition (Fig. 11).

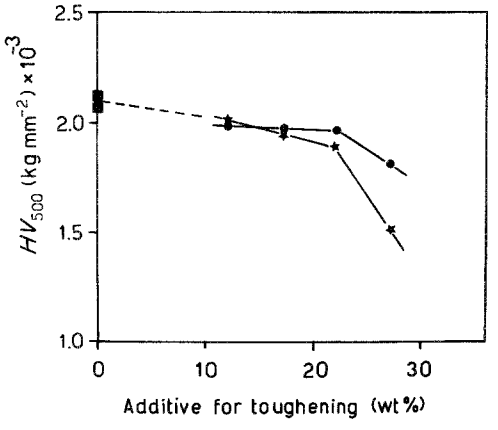

Figure 7 Variation of Vickers microhardness with the amount of ZrO_2 in materials of the Si_3N_4–MgO–ZrO_2 system. The two lines refer to different grain sizes of ZrO_2 powder with BET surface areas of (●) 3.9 and (★) 8.0 m^2 g^{-1}. All samples had 3 wt % MgO.

3.3.3. Kick's analysis modified according to Hays and Kendall

Kick [13] proposed analysing the results on hardness with a relation between the load P and the indentation length d similar to Equation 1:

$$P = K_1 d^n \qquad (2)$$

but he postulated a constant value for n equal to 2 for all indentors and for all geometrically similar impressions. As already shown, and deducible from Figs 8 and 9, these statements are not confirmed by the materials examined by us. Hays and Kendall [14] attempted to overcome this difficulty by assuming that the resistance to deformation could be evaluated by considering it as a Newtonian resistance pressure of the specimen itself. As a load P is applied to a crystal sample, they assumed that the value of P is partially affected by a small resistance pressure W which is a function of the material being tested. W could represent the minimum applied load needed to produce an indentation, since the load W allows no plastic deformation. On the basis of this hypothesis, Equation 2 is modified to

$$P - W = K_2 d^2 \qquad (3)$$

which, using Equation 1 for which the constants were already calculated for each material examined,

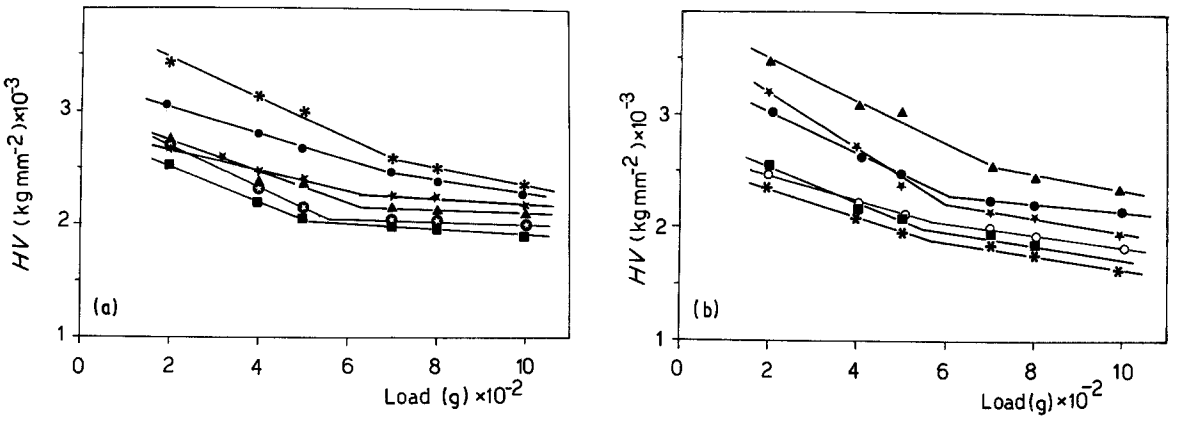

Figure 8 Vickers microhardness of the applied load (10 sec indentation time). (a) Si_3N_4–Al_2O_3 and Si_3N_4–MgO systems: (*) A1, (★) A2, (▲) A3, (●) M1, (○) M2, (■) M3. (b) Si_3N_4–Al_2O_3–ZrO_2 system: (▲) AZ1, (★) AZ2, (●) AZ3, (○) AZ4, (■) AZ5, (*) AZ6.

becomes

$$d^n = \frac{W}{a} + \frac{K_2}{a} d^2 = B_1 + B_2 d^2 \qquad (4)$$

The graphical representation of Equation 4 is shown in Fig. 12 and it is evident that this equation may represent the experimental data. All the materials considered, apart from the chemical composition and the microstructural characteristics, converge to the same value of the constant B_1, while the B_2 constant remains the specific characteristic of each material.

The W values range from 50 to 80 g depending on the material and, as shown for the parameter a (Fig. 11), they can be related to the grain size. The B_2 constant does not seem to be directly related to each microstructural parameter of the tested materials. It seems therefore appropriate for a general representation of the material.

4. Conclusions

Small variations in the concentration of densification aids or the additive type strongly affect the microhardness of β-Si_3N_4-based ceramics produced by hot pressing. The presence of intergranular glassy phases generally lowers the microhardness. On the other hand, a more crystalline intergranular phase gives rise to relatively higher microhardness values. The highest microhardness was recorded in samples with a very low content of intergranular phase (materials of the Si_3N_4–Al_2O_3 and Si_3N_4–Al_2O_3–ZrO_2 systems). The compositional ranges of the tested materials proved to be useful to investigate the change in microhardness for dense Si_3N_4 ceramics prepared with various polyphase microstructures (glassy or crystalline intergranular phase, toughening phase). The microhardness of silicon nitride-based materials may also be related to some microstructural parameters such as porosity, mean grain size and residual α-Si_3N_4 phase.

Furthermore, a comparative analysis of different materials cannot exclude the microhardness tests in a wide range of values of the applied load during the indentation, with a Newtonian resistance which value is specific for each material. The investigation of the Meyer and of the Kick models allows one to obtain the relation

$$d^n = B_1 + B_2 d^2$$

where the constant B_1 may represent a class of

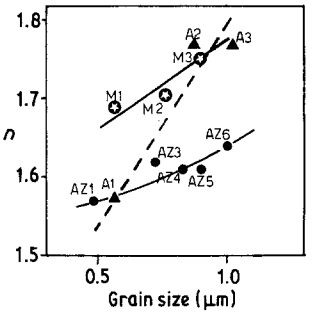

Figure 10 Dependence of slope of Meyer lines on grain size for the materials tested.

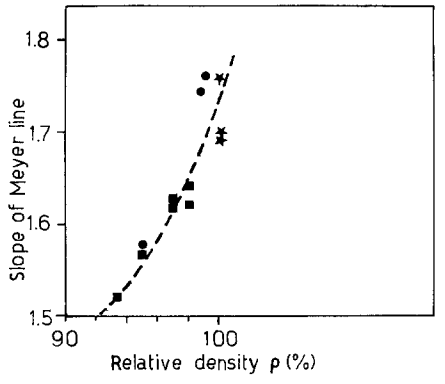

Figure 9 Slope of Meyer line against relative density: (■) Si_3N_4–Al_2O_3–ZrO_2, (●) Si_3N_4–Al_2O_3, (★) Si_3N_4–MgO.

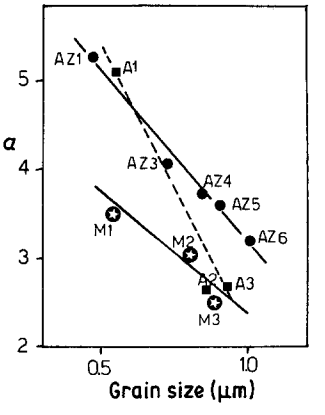

Figure 11 Dependence of the intercept of Meyer lines on grain size for the materials tested.

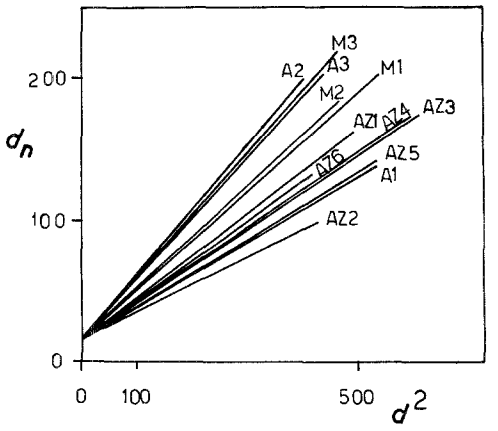

Figure 12 Plot of Equation 4 showing that this equation may represent all the experimental data.

materials, while the constant B_2 is specific for each single material.

References

1. N. L. PARR, G. F. MASTIN and E. R. W. MAY, in "Special Ceramics", edited by P. Popper (Haywood, London, 1960) p. 102.
2. P. B. NOAKES and P. L. PRATT, in "Special Ceramics 5", edited by P. Popper (British Ceramic Research Association, Stoke-on-Trent, 1972) p. 229.
3. R. F. COE, R. J. LUMBY and M. F. PAWSON, *ibid.* p. 361.
4. K. NIHARA and T. HIRAI, *J. Mater. Sci.* **13** (1978) 2277.
5. D. CHAKRABORTY and J. MUKERJI, *ibid.* **15** (1980) 3051.
6. A. TSUGE and K. NISHIDA, *Amer. Ceram. Soc. Bull.* **57** (1978) 424.
7. C. GRESKOVICH and H. C. YEH, *J. Mater. Sci. Lett.* **2** (1983) 657.
8. K. TSUKUMA, M. SHIMADA and H. KOIZUMI, *Amer. Ceram. Soc. Bull.* **60** (1981) 910.
9. F. Z. MEYER, *Vereins Deut. Ing.* **52** (1908) 52.
10. *Idem, ibid.* **52** (1908) 645.
11. *Idem, ibid.* **52** (1908) 740.
12. *Idem, ibid.* **52** (1908) 835.
13. F. KICK, "Das Gesetzder, Proportionalen Winderstande und Science answendung" (Felix, Liepzig).
14. C. HAYS and E. G. KENDALL, *Metallography* **6** (1973) 275.
15. G. N. BABINI, A. BELLOSI and P. VINCENZINI, paper presented at the 86th Annual Meeting of The American Ceramic Society, Pittsburgh, 1984 (unpublished).
16. *Idem*, Internal Report CNR-IRTEC 84/243 (unpublished).
17. G. N. BABINI, A. BELLOSI, R. CHIARA and M. BRUNO, paper presented at Special Ceramics 8 (London, 18–20 December, 1985).
18. G. N. BABINI, A. BELLOSI and P. VINCENZINI, *Ceramurgia* **14** (1984) 51.
19. *Idem, Ceramurgia Int.* **3** (1980) 91.
20. *Idem, Mater. Chem. Phys.* **11** (1984) 365.
21. *Idem, J. Amer. Ceram. Soc.* **64** (1981) 578.
22. *Idem*, in "Science of Ceramics 12," edited by P. Vincenzini (Ceramurgica, Faenza, 1984) p. 471.
23. *Idem, J. Mater. Sci.* **19** (1984) 1029.
24. *Idem, ibid.* **19** (1984) 3487.

Received 16 June
and accepted 18 August 1986